Friction

Research Article

Active control of friction in electrified ball bearing prototypes using electro-sensitive clay mineral-based lubricating fluids

Samuel David Fernández-Silva[1], Miguel Ángel Delgado[1], Claudia Roman[1], Tobias Amann[2,3], Felix Gatti[2,3], Andreas Kailer[2], Moisés García-Morales[1,✉]

Cite this article: Fernández-Silva SD, Delgado MA, Roman C, et al. *Friction* 2025, **13**: 9441023. https://doi.org/10.26599/FRICT.2025.9441023

ABSTRACT: The aim of this research is to present the use and advantages of electro-active eco-fluids as smart biolubricants. Polarizable clay mineral nanoparticles, such as the layered nanosilicate montmorillonite Cloisite 15A and the fiber-like sepiolite Pangel B20, were dispersed in a sustainable fluid, castor oil, at concentrations of 0.5, 2, and 4 wt%. These dispersions exhibit electro-viscous behavior, which was characterized by higher yield stress values with increasing electric field strength. Based on this, the influence of electric potentials was investigated in an electrified axial ball bearing device. The coefficient of friction (COF) was changed as needed and reversibly when different electric fields of 100 and 200 V/mm were applied. A 10.7% increase in the coefficient of friction was observed with a 4 wt% Cloisite 15A in castor oil at 200 V/mm. In the case of Pangel B20, the application of an electric field of 200 V/mm successfully prevented the lubricant from being displaced from the contact zone at 500 r/min. In addition, the dielectric breakdown resistance of these clays was analyzed. Cloisite 15A yielded better results than Pangel B20, probably due to its greater electro-responsive and thus film-forming potential. Finally, the load-carrying capacity was also evaluated. Under the action of an electric field, an opposite vertical force was observed when a ball was pressed onto a plate with a lubricating film in between. Consequently, the study allows conclusions to be drawn about a new lubrication concept based on electro-active control of friction in electrified tribological contacts by fully sustainable electro-rheological (ER) lubricating fluids.

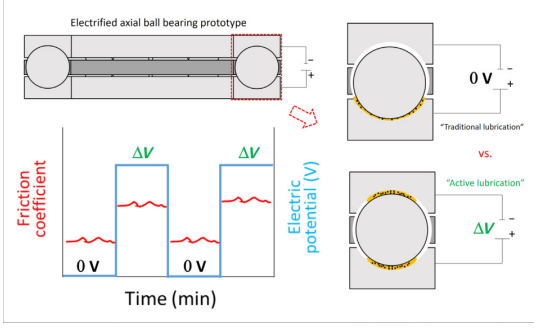

KEYWORDS: smart lubricant; sustainability; ball bearing; active control of friction; nanoclay mineral

1 Introduction

Energy consumption due to human activity is increasing daily. Energy and resources savings and reducing pollution have emerged as some of the most important global challenges, as reported in the "The Global Sustainable Development Report (GSDR) 2023" of the United Nations Organization. Considering that around 23% of the current energy consumption was related to friction [1], reducing contact friction can increase efficiency in engines and other friction-involved applications [2], which may contribute to reduce fuel consumption and pollution emission to the environment. On the other hand, wear, the other important aspect in tribological contacts, affects the durability of the mechanical elements involved. Upon failure, they need replacing to continue to operate. Production of metal parts is commonly associated to CO_2 emissions. Therefore, a joint reduction of friction and wear would greatly help reduce global warming [3].

The search for new materials sources is also a key factor in addressing the environmental issues mentioned above. Usage of sustainable oils is currently gaining popularity. Among them, vegetable oils stand out for their good lubricating properties. One of them, castor oil, has been widely studied due to its uniquely high viscosity, and has been proposed as a potential lubricant base stock [4, 5]. Vegetable oils are also known to be an excellent alternative to mineral oils in preventing the harmful voltage breakdowns [6]. Although they are good candidates, they have not yet replaced mineral/synthetic oils in lubrication due to critical chemical factors such as oxidation and low range of viscosities available, which limit the maximum operating temperature [7, 8].

Achieving *in situ* control of friction is an important challenge for the lubrication industry nowadays [9]. Some authors are currently engaged in investigations that aim to enable an active or programmed lubrication control. Different types of ionic liquids (ILs) have been widely studied due to the capacity of their ionic

[1] Departamento de Ingeniería Química, Centro de Investigación en Tecnología de Productos y Procesos Químicos (Pro2TecS), Campus de "El Carmen", Universidad de Huelva, 21071, Huelva, Spain. [2] Fraunhofer Institute for Mechanics of Materials IWM, MicroTribology Center μTC, Woehlerstraße 11, 79108 Freiburg, Germany. [3] Fraunhofer Cluster of Excellence Programmable Materials CPM, Woehlerstraße 11, Freiburg 79108, Germany.

✉ Corresponding author. E-mail: moises.garcia@diq.uhu.es

Received: September 19, 2023; Revised: February 9, 2024; Accepted: October 14, 2024

moieties to be approached and molecularly layered by charged surfaces, and hence to modify friction [10–13]. For instance, Gatti et al. [11] used a mixture of two ILs, (trihexyltetradecyl-phosphonium-bis(trifluoromethylsulfonyl)-imide [P66614][BTA] and trihexyltetradecylphosphonium-bis(2-ethylhexyl)-phosphate [P66614][DEHP]), in different proportions to program friction values throughout time with the application of anodic and cathodic polarization. Other types of strategies, based on self-assembled monolayer (SAM) assemblies [14] or polyelectrolyte coatings [15], are being used with the same purpose. The study of all these surface modifications by the action of an electric field is referred to by the terms "triboelectrochemistry" [16] and "potential controlled friction (PCF)" [17]. Moreover, the integration of electronics in the active control of all these lubrication processes has been coined "tribotronics" [16, 18], and the fluids involved are frequently called "smart" lubricants [18]. In this sense, electro-rheological (ER) and magneto-rheological (MR) fluids have been proposed as possible smart lubricants to control the tribological behavior. These fluids are designed to respond to a determined external driving force, electric or magnetic field, respectively, in such a way that their rheological properties change substantially [18, 19]. MR fluids have been widely tested and showed some promising results with possibilities to control friction and reduce wear [19]. In the case of ER fluids, especial emphasis has been placed on liquid crystals, which have been shown to yield noticeable decrease in the friction coefficient in boundary regimes [20]. Regarding particle-in-oil ER suspensions, there are published articles dealing with numerical simulations in simple journal bearings using a lubricant which is modelled as a Bingham fluid [21, 22]. However, only scarce literature, none of them involving sustainable fluids, exists on the active control of friction through real ER suspensions under an electric field.

Despite all these relevant advances in the control of friction, ER lubricants require an electric field to function. Another important aspect of smart lubricants is the prevention of unwanted or uncontrolled current flow through contact surfaces exposed to an external electric field. Liquids that are too conductive lead to undesirable electrical current leakage. Even in dielectrics, if the input voltage is too high, a sudden electrical discharge can occur between the electrified elements. This phenomenon, which is known as dielectric breakdown, depends on both the lubricant intrinsic properties [23] and the film thickness. Dielectric breakdown may yield severe damage on the bearing cage and balls due to electrical pitting [24], which may eventually cause vibrations and noise.

In a previous paper, we carried out an electro-rheological characterization on 2 wt% nanoclay mineral particles in castor oil [25]. The organo-modified montmorillonite Cloisite 15A and the sepiolite Pangel B20 were found to yield storage stable formulations in castor oil. Cloisite 15A suspensions showed higher ER performance, assessed by their yield stress values at 25 °C. This was related to a local maximum in the dielectric loss curve, ε'', in the frequency range of 5–10 kHz, which was attributed to interfacial polarization. Hence, the mentioned research focused on exploring the development of simple and sustainable lubricants, based on nanoclay mineral particles in vegetable oil, which might enable an "active control" of their tribological behavior. However, such approach lacked an experimental study on the use of the obtained formulations in specialized tribological applications such as ball bearings, and the potential drawbacks which might arise.

In line with the above comments, the present study aims to look into the potential use of such ER fluids, based on completely natural and innocuous compounds, as smart lubricants capable of actively modifying friction, preventing unwanted discharges, and supporting heavier loads in electrified ball bearing contacts. Our strategy ensures environmental protection, which is an important aspect in various fields in which the machinery may be in direct contact with the natural medium, i.e., marine propulsion, wind turbines, etc. [2, 26]. We hypothesize that it is feasible to improve the performance of ball bearings, in terms of better stability at high speeds, by electro-active control of lubrication with sustainable ER fluids.

2 Materials and methodology

2.1 Materials

Oil-based dispersions of two commercially available nanoclays, Cloisite 15A and Pangel B20, were evaluated in this study. Cloisite 15A is a layered organomodified montmorillonite (OMMt) formed by two tetrahedral sheets of silicon and oxygen, and one octahedral sheet of Al/Mg(OH) in between [27] (Fig. 1(a)). The distance between the layers is 31.5 Å. Interlayered sodium ions were replaced with quaternary ammonium salt cations to improve their dispersibility in oil. The organic part of the modifier is 2Me2HT (Me: methyl and HT: hydrogenated tallow (~65 wt% C18; ~30 wt% C16; ~5 wt% C14)). Cloisite 15A was supplied by Southern Clay Products, USA.

Pangel B20 is a fiber-like sepiolite composed of a sandwich-like structure of two tetrahedral sheets of silicon and oxygen (silica) and an interlayered octahedral sheet of magnesium oxide hydroxide. Silica layers are covalently bonded by oxygen atoms to form ribbons (Fig. 1(b)). These units bundle to form a fiber-like structure with zeolitic channels of 3.7–10.6 Å. Due to their open structure, silanol groups remain in the borders of the silica, thus coordinating with water molecules [28–30]. Pangel B20 was supplied by Tolsa, Spain.

Castor oil (CO), with dynamic viscosity at 25 °C of 0.69 Pa·s, was employed as base oil for the preparation of the dispersions. CO was purchased from Guinama, Spain.

2.2 Preparation of sustainable lubricating dispersions

The nanoclays were firstly pre-dispersed in castor oil by mechanical stirring at room temperature. Subsequently, the dispersions were treated with an ultrasonic homogenizer (UP400St, Hielscher, Germany), supplying a total energy input of

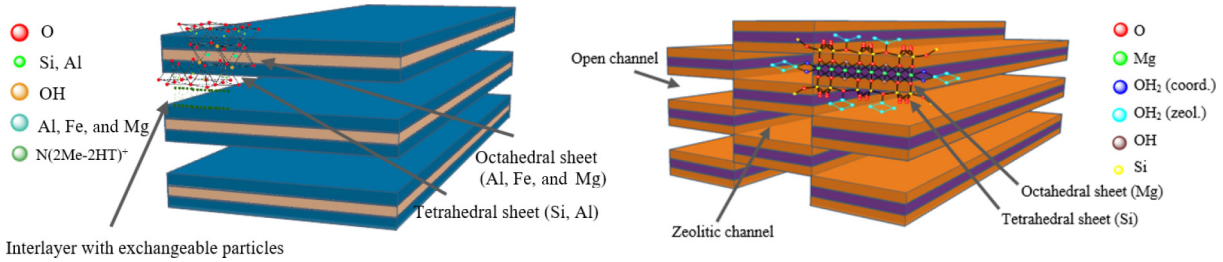

Fig. 1 Structures of (a) montmorillonite Cloisite 15A and (b) sepiolite Pangel B20.

7 Wh each. Temperature was always kept below 75 °C. Concentrations of 0.5, 2, and 4 wt% were studied. By following this method, very homogeneous dispersions were achieved. Their storage stability was analyzed by sedimentation tests (in test tubes) in a previous paper [25]. The results obtained allowed concluding that the dispersions remained storage-stable after, at least, 7 days.

2.3 Electro-rheological characterization of sustainable lubricating dispersions

Steady viscous flow curves at 25 °C were performed at increasing values of the DC electric field up to 2.4 kV/mm, in a shear rate interval from 0.1 to 100 s^{-1}. A controlled rate rheometer (ARES G2, TA Instruments, USA), equipped with a special electro-rheocell, a electric field generator (Keysight 33210A, Agilent, USA) and a high-voltage power amplifier (Trek 609E-6, Trek Inc., USA), was used. A plate-plate geometry with 25 mm diameter and 0.5 mm measuring gap was selected. Additionally, such a set-up was also used to evaluate the electrical conductivity of the fluids by applying, under quiescent conditions, a voltage ramp up to 100 V whilst the electric current intensity was measured. The electrical conductivity values, at 25 °C, corresponding to the above Cloisite 15A and Pangel B20 dispersions, at concentrations between 0.5 and 4 wt%, fall within the intervals (4.20×10^{-11}–1.69×10^{-10} and 3.05×10^{-11}–2.37×10^{-10} S/cm, respectively.

2.4 Electro-tribological analysis of sustainable lubricating dispersions in electrified ball bearings

A controlled stress rheometer (Physica MCR-501, Anton Paar, Austria) equipped with a customized ball bearing arrangement (Fig. 2(a)) was used for friction and breakdown resistance measurements. A voltage generator (9183B, BK Precision Corp, USA), and a potentiostat-galvanostat (Parstat 4000A, Ametek, USA) were coupled to the rheometer for precise control of voltage up to 10 and 20 V, respectively. For higher voltages, up to 1,000 V, a generator (FUG 12500, FUG, Germany) was preferred. An oscilloscope (Picoscope 3000, Pico Technology, UK) was used to record voltage and current.

A controlled rate rheometer (ARES-G2, TA Instruments, USA) was used for film strength measurements, where a current generator (Keysight 33210A, Agilent, USA) connected to a voltage amplifier (Trek 609E-6, Trek Inc, USA) allowed for the application of the electric fields required. The structuring of Cloisite 15A and Pangel B20 into strings under the influence of electric field was analyzed using a home-made visualization device coupled to an optical microscope (Olympus BX51, Olympus, Japan). The visualization device was based on two electrodes, between which the lubricant is located, connected to the aforementioned electric field generator and placed under the lens of the microscope.

2.4.1 Analysis of the active control of the friction coefficient

The tests were performed with an electrified ball bearing assembly like one of the prototypes described in US 2010/0247012 A1 [31]. An axial ball-bearing (DIN 51104) with ball radius of 5.55 mm (7/32 inch), was arranged with 13 Si_3N_4 ceramic balls (Fig. 2(a)), resulting in a hybrid bearing. The ceramic balls isolated the two electrified rings, thus enabling the application of high voltages without the risk of shortage. Tests were conducted at voltages up to 1,000 V, rotating speeds up to 1,000 r/min and constant normal load of 5 N.

2.4.2 Evaluation of the dielectric breakdown resistance of the lubricant

Breakdown occurs when the fluid no longer maintains its dielectric properties, thus current starts passing through the lubricant film (the oscilloscope registers both a sharp decrease in the voltage and a peak in the electric current intensity). In this test, one of the isolating ceramic balls in Fig. 2(a) was replaced with a conductive steel ball. Tests were conducted at 1,000 r/min and 5 and 10 N. Stabilization of the friction coefficient was carried out during the first 5 to 10 min, with no application of electric voltage. Once stabilized, electric voltage was increased in steps of 0.1 V from 0 to 20 V until electric arc detection.

2.4.3 Study of the load-carrying capacity of the lubricant film under electric field

A steel ball (1.4401 grade 100) with a radius of 6.35 mm approached a steel plate (1.4301 AISI 304), at a speed of 0.5 μm/s from an initial distance of 0.3 mm down to 0 mm (or minimum achievable distance). Both ball and plate were electrified (Fig. 2(b)). The purpose of this experiment was to determine whether upward forces are generated in the lubricating film under the influence of the external electric field, which oppose the moving plate.

3 Results and discussion

3.1 Electro-active control of the friction coefficient

Figure 3 shows the electro-rheological behavior, at 25 °C, for 2 wt% nanoclay in castor oil, as a function of electric field strength. The electroviscous effect observed is based on the so-called interfacial (or Maxwell-Wagner) polarization upon application of a potential difference. Such type of polarization refers to the phenomenon of charge separation at the interfaces of two media (in this case, nanoclay and oil) having different dielectric constant. As a result, chain-like structure is formed bridging both electrodes along which the electric field is applied, thereby yielding a very noticeably increase in the shear stress value that is needed before the material starts flowing. With increasing the electric field strength the polarization state of the nanoparticles increases, thereby yielding stronger linkages between the units that constitute the string-like structure. As a proof of it, a video showing the string-like structure formation of Cloisite 15A and Pangel B20 in castor oil is provided as Electronic Supplementary Material (ESM) (available from https://video.uhu.es/media/

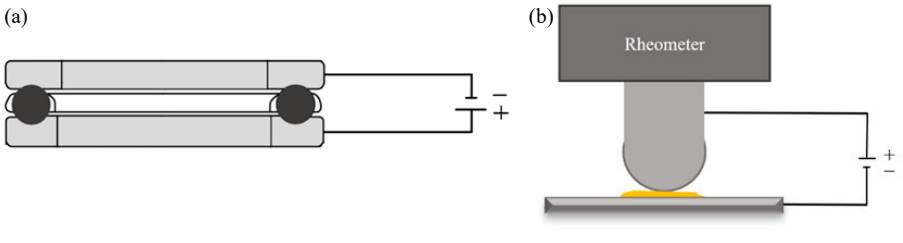

Fig. 2 (a) Ball bearing assembly consisting of two electrified cages and insulating ceramic balls. (b) Ball-on-plate configuration.

清華大学出版社 Tsinghua University Press | SciOpen

t/1_8gkjbs0c). As can be appreciated, despite its Newtonian behavior at 0 V, Cloisite 15A dispersion exhibits a larger electro-rheological potential than Pangel B20 dispersion. An increase in viscosity at 0.1 s^{-1} by two and a half decades was observed for Cloisite 15A when 2.4 kV/mm was imposed. In contrast, for Pangel B20, which exhibits a strong pseudoplastic character at 0 V, the viscosity at low shear rate (0.1 s^{-1}) could be increased by only one decade by the electric field. These results demonstrate the greater electro-viscous potential of the layered nanosilicate Cloisite 15A. For example, 2 wt% Cloisite 15A in castor oil displayed a low shear rate viscosity of 6×10^2 Pa·s at 2.40 kV/mm, as compared to 2 wt% Pangel B20 in castor oil with a low shear rate viscosity of only 10^2 Pa·s (limiting value). The results also prove the extraordinary intrinsic thickening capacity of the sepiolite Pangel B20.

The electrorheological potential of such dispersions opens the possibility of electro-active control of friction in electrified tribological contacts by fully sustainable ER lubricating fluids. Based on this, electrical voltages up to 1000 V were applied to the electrified ball bearing set-up shown in Fig. 2(a). Friction coefficient vs. time is represented in Fig. 4 for dispersions of both types of nanoclay, as a function of concentration (0.5, 2, and 4 wt%). Testing conditions included a normal force of 5 N and rotating speed of 500 r/min. Two different voltages of 500 and 1000 V were applied in two periods of 400 s, with an intermediate interval of 300 s with no electric field. With a distance between the bearing rings (electrodes) of 5 mm, electric fields of 100 and 200 V/mm were obtained.

Before analyzing the electro-active control of the friction process, the effect of nanoparticle concentration on the coefficient of friction (COF) should be discussed. The ball bearing tests were carried out in the hydrodynamic lubrication regime. Such a lubrication regime is characterized by contact surfaces being fully separated by a relatively thick film of lubricant. Hence, the COF increases as the lubricant viscosity is increased. Cloisite 15A in castor oil exhibited Newtonian behavior, with viscosity at 25 °C gradually increasing from 0.69 Pa·s (pure castor oil) to 1.07 Pa·s upon addition of 4 wt% Cloisite 15A. Therefore, in the absence of electric voltage, the observed increase in COF with concentration is attributed to the increase in the biolubricant dynamic viscosity. For Pangel B20, only minor differences of less than 2% in COF were observed between 0.5 and 2 wt% at 0 V. Despite the differences observed in their shear-thinning behaviors with concentration, such dispersions showed a similar limiting viscosity at very high shear rates. This agrees with the result in Fernandez-Silva et al. [32]. In addition, it is noteworthy that due to the high thickening capacity of this type of sepiolite, the 4 wt% dispersion behaved like a very consistent semisolid liquid (comparable to a conventional lubricating grease with NLGI 2 or 3). As a consequence, part of the lubricant was already ejected in the initial phase of the test due to the high centrifugal forces in the ball bearing. This caused lack of lubricant in the contact surface.

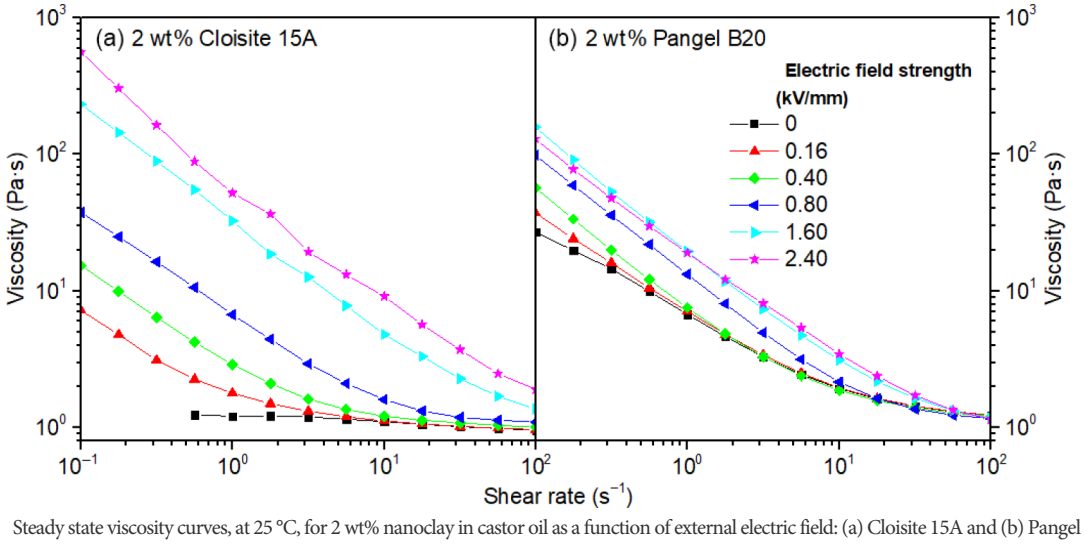

Fig. 3 Steady state viscosity curves, at 25 °C, for 2 wt% nanoclay in castor oil as a function of external electric field: (a) Cloisite 15A and (b) Pangel B20.

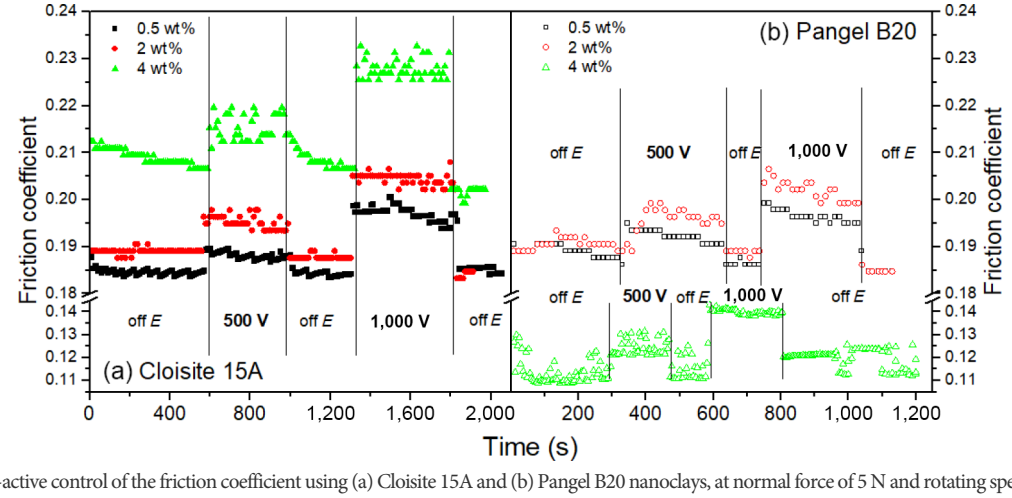

Fig. 4 Electro-active control of the friction coefficient using (a) Cloisite 15A and (b) Pangel B20 nanoclays, at normal force of 5 N and rotating speed of 500 r/min.

Under hydrodynamic regime conditions, at which the tests were conducted, lubricant viscosity is the main factor governing the frictional behavior, given that the solid surfaces are sufficiently apart such that solid friction does not occur. In consequence, starved lubrication is expected to yield a lower COF value than fully flooded lubrication. As a result, an anomalous reduction in the hydrodynamic COF was obtained (Fig. 4(b)), which can be attributed to starved lubrication. For the sake of reference, it is noteworthy that the corresponding "dry" lubrication curve (total absence of lubricant) yielded a COF value of ca. 0.01. On the other hand, it is also important to note the appearance of vibrations and noise in the ball bearing at such concentration.

The application of an external electric field enabled the COF to be actively adjusted on demand. With the exception of the 4 wt% Pangel B20 dispersion, which resulted in starved lubrication, all tests were conducted under fully flooded conditions. Under comparable fully flooded lubrication conditions, i.e., at 0.5 and 2 wt%, Cloisite 15A and Pangel B20 yielded similar COF variations at 500 V (100 V/mm), while Cloisite 15A gave only slightly larger COF variations at 1,000 V (200 V/mm). Thus, the COF behavior does not seem to strictly follow the electro-rheological pattern depicted in Fig. 3. Mechanisms other than the pure electro-viscous effect appear to be involved in lubrication performance. Consequently, the results from electro-rheological measurements cannot be directly extrapolated to the electro-tribology issue. In addition, the COF returned to its initial value after the electric field was turned off, demonstrating the immediate reversibility of this electro-active control of the viscosity of the biolubricant.

Moreover, Fig. 5 displays the evolution of current intensity with time for the above described electro-active control tests in an electrified ball bearing prototype, at two selected nanoclay concentrations (0.5 and 2 wt%). Current flow increased with both electric potential and concentration. As expected from the low conductivity values above reported, small current flow values, in the order of hundreds of μA, were found even at the largest value of applied voltage, 1,000 V. As previously mentioned, it is worth noting the importance of low leakage current in practical applications of ER fluids as smart materials. Low conductive fluids prevent short circuit and help minimize the unwanted large power consumption. Current intensity values were not significantly different between nanoclays, and were found to remain constant with time. However, at 1,000 V, the signal was notoriously affected by noise, mainly that corresponding to Pangel B20. This fact might be related to the stability of the lubricant film.

Table 1 lists the percent increase in COF as a function of applied voltage and concentration. In general, COF increased with concentration. At 1,000 V, the use of Cloisite 15A at concentrations up to 2 wt% caused a greater increase in COF than with Pangel B20. At 4 wt%, Pangel B20 caused an increase in COF, which is probably due to the starved lubrication mentioned above.

With hydrodynamic lubrication, almost no wear occurs as long as the contacts are sufficiently lubricated. Under such circumstances and for smart lubricant applications, the lubricant viscosity should be reduced to optimal values, as reported by Barber et al. [33]. Nevertheless, such electro-active control offers the unique opportunity to adjust the lubricant viscosity by means of electrical voltages in such a way that it can optimally adapt to different load conditions. This enables the lubricity of the same biolubricant to be adapted to changing working conditions, reducing the need for often very hazardous additives to improve lubricity, friction, and viscosity index. In a further development, the electro-sensitive potential of these biolubricants could help mitigate other negative effects caused by high speeds, for example.

Figure 6(a) shows the fluid leakage from the axial ball bearing when it was lubricated with 4 wt% Pangel B20 in castor oil without electric field. The high viscosity of the dispersion leads to

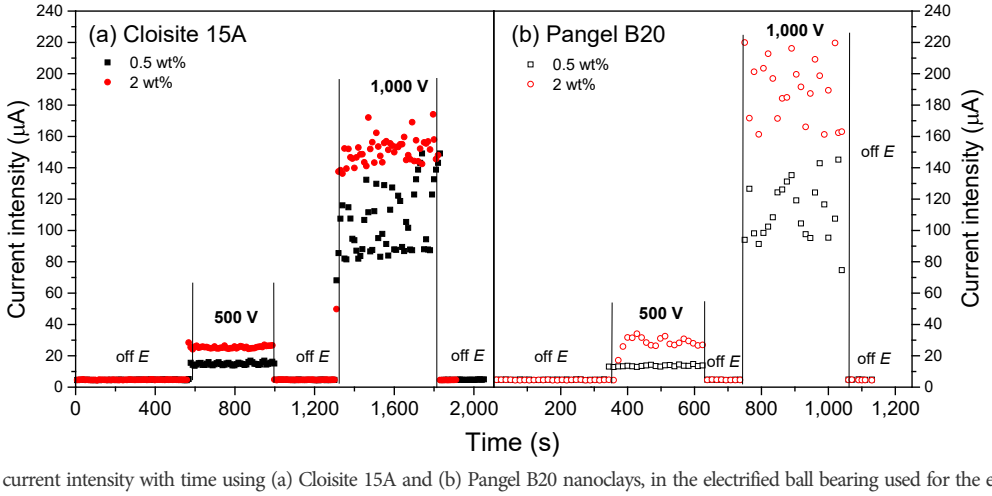

Fig. 5 Evolution of current intensity with time using (a) Cloisite 15A and (b) Pangel B20 nanoclays, in the electrified ball bearing used for the electro-active control study.

Table 1 Percentage increase (%) in COF with the application of electric fields of 500 and 1,000 V

	Conc. (wt%)	0 to 500 V	0 to 1,000 V
15A	0.5	3.1	8.6
	2	3.7	9.8
	4	4.0	10.7
B20	0.5	3.1	5.5
	2	3.8	8.5
	4	5.5	25.4

poor wetting of the contact zone, resulting in starved lubrication when the biolubricant is partially expelled at 500 r/min without external electric field. This undesirable phenomenon was reversed when a potential difference of 1,000 V was applied from the start of the test so that the lubricant could no longer be expelled (Fig. 6(b)). At higher rotating speeds than 500 r/min, lubricant expulsion continued to occur, indicating that a higher voltage is probably required to keep the lubricant in the contact zone. For the sake of clarity, a video is provided as ESM (available from https://video.uhu.es/media/filmora%20articulo%20v2.mp4/1_lpm4z48j).

In addition, the insets in the lower right corner of Fig. 6 show the COF stabilization process for the 4 wt% Pangel B20 in castor oil at a rotation speed of 500 r/min. At 0 V, COF remained unstable within the whole period elapsed. A deep resonating noise was perceived during the entire test period. However, when the same test was performed under 1,000 V, the COF leveled off noticeably fast and remained stable. Moreover, the noise disappeared. It seems that the electric field forces the surrounding oil-wetted electro-sensitive Pangel B20 nanoparticles to concentrate in and around the region where the electric field strength is highest, i.e., at the contact point between the sphere and the ring. The nanoparticles shield the oil from leaking and thus improve lubrication. This is in contrast to reports of oils that do not contain ER particles [34]. After the electric field was turned off, the lubricant seemed to remain for a while in the contact zone (transient polarization state of the nanoparticles) [35], until it was finally ejected by centrifugal forces. Therefore, we can conclude that the amount of biolubricant needed to keep the friction stable could be reduced through the proposed strategy of smart electro-responsive lubrication.

3.2 Dielectric breakdown analysis in an electrified ball bearing

The ball bearing configuration described in Section 2.4.1, with 12 isolating ceramic balls and one conductive steel ball, was used for the analysis of lubricant breakdown resistance, in accordance with the technique described in Jablonka et al. [36] and later improved by Shetty et al. [37] for evaluating this phenomenon in rolling bearings. Tests were conducted under normal forces of 5 or 10 N and a rotating speed of 1,000 r/min (approximate entrainment speed of 1.25 m/s). The purpose of this test was to investigate how the electro-active control of the lubricant film may affect the dielectric breakdown when ER fluids are used in ball bearings.

Table 2 shows the dielectric breakdown voltages for both Cloisite 15A and Pangel B20 dispersions at the three concentrations studied. Note that displayed values were measured under the real working conditions specified in Section 2.4.2 (different from ASTM D877 and ASTM D1816). Technical limitations of the measuring device (maximum measurable voltage of the oscilloscope was 20 V) prevented the breakdown from being detected when the tests were performed under a normal force of 5 N. As a result, it was not possible to perform a comparative analysis between the nanoclay types under these force values. Tests were then performed under less favorable loading conditions, i.e., 10 N. With addition of 0.5 wt% Cloisite 15A, the breakdown resistance of the base castor oil was enhanced, yielding an increase from 1.4 to 7.4 V. Concentrations of 2 wt% or more could delay breakthrough beyond 20 V. It seems that the Cloisite 15A nanoclay improves the lubricating film formation, probably due to its very high electro-responsive capacity, as shown in Fig. 3. This had a positive effect on the load carrying capacity of the biolubricant under an external electric potential (Section 3.3). Although the Pangel B20 dispersions exhibited distinctly grease-like behavior, the electro-responsive capacity of Pangel B20 was not large enough for this nanoclay to remain at the contact point at the low voltages used in this test. Thus, even at 4 wt%, the lubricant was not able to significantly improve the film formation of neat castor oil, so that an electrical shorting (current leakage) occurred at about 2 V.

Based on the above considerations, the theoretical minimum gap within the lubricated contact in the hydrodynamic regime

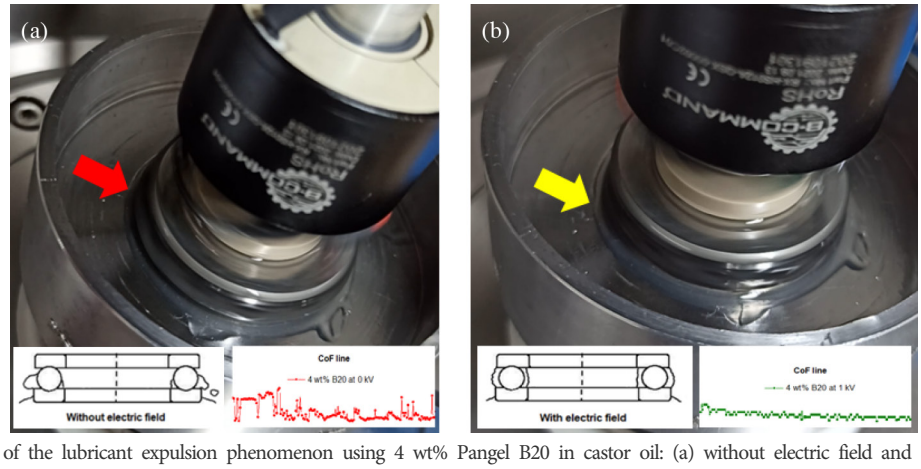

Fig. 6 Visual evidence of the lubricant expulsion phenomenon using 4 wt% Pangel B20 in castor oil: (a) without electric field and (b) applying an external voltage of 1,000 V.

Table 2 Dielectric breakdown voltages (in V) measured as described in Section 2.4.2, for Cloisite 15A and Pangel B20 in castor oil

Conc. (wt%)	5 N		10 N	
	15A	B20	15A	B20
0 (neat oil)	19.4	19.4	1.4	1.4
0.5	>20	>20	7.4	1.5
2	>20	>20	>20	1.8
4	>20	>20	>20	2.1

(i.e., minimum film thickness (H_m)) was calculated using the Hamrock–Dowson model (Eq. (1)) [38–40]:

$$H_m/R_x = 3.63 \cdot G^{0.49} \cdot U^{0.68} \cdot W^{-0.073} \left(1 - e^{-0.68k}\right) \quad (1)$$

where $k = 1$ for a ball on plain surface (k is the ellipticity parameter, defined as the ratio of the radii of curvature of the contacting surfaces in the direction of the major and minor axes of the contact ellipse) ; G, U, and W are dimensionless parameters of the Hamrock–Dowson equation (Eqs. (2)–(4)):

$$G = \alpha_p \cdot E' \quad (2)$$

$$U = \frac{\eta \cdot u}{E' \cdot R_x} \quad (3)$$

$$W = \frac{F}{E' \cdot R_x^2} \quad (4)$$

where α_p (Pa^{-1}) is pressure-viscosity coefficient (14.2 GPa^{-1} [41, 42]); E' (Pa) is equivalent elastic constant from 100Cr6 steel elasticity modulus (210 GPa); η (Pa·s) is viscosity (measured values at 0.5, 2, and 4 wt% were 0.84, 0.96, and 1.07 Pa·s, respectively); u (m/s) is entraintment speed; F (N) is load; R_x is curvature radius (ball radius).

Table 3 shows the minimum film thicknesses calculated according to Eq. (1) for the three Cloisite 15A dispersions investigated. Neat castor oil was included as control sample. For a comparative analysis, the experimentally measured breakdown voltages were color-coded in Table 3 (potential intervals are marked with different colors). As can be observed, neat oil failed to prevent breakdown even at the largest entrainment speed studied, i.e., 2.75 m/s. However, with increasing Cloisite 15A concentration, the onset of each specific breakdown voltage interval was reached at smaller entrainment speeds.

Thus, the speed at which the orange voltage interval (breakdown voltage between 5 and 10 V) started was reduced from 1.25 to 0.75 m/s as Cloisite 15A concentration was raised from 0.5 to 4 wt%. At 2 and 4 wt% Cloisite 15A, the lubricant film thickness bounding the red, orange, and grey breakdown voltage intervals decreased with increasing concentration. It is expected that future work on this topic will yield a relationship between the concentration, velocity, and thickness of the film that will efficiently predict the occurrence of electrical breakdown.

To further investigate the fundamentals of the lubrication mechanism, a 2 wt% Cloisite 15A in castor oil formulation was visualized under an electric field of 2.4 kV/mm in the optical cell. It has been shown that despite the electronegative character usually attributed to clay minerals, the metal plate acting as a negative electrode attracts the nanoparticles, forming a protective layer (Fig. 7(a)). Montmorillonite nanoplatelets organomodified with cationic surfactants have been shown to exhibit positive zeta potential [43]. Accordingly, a possible explanation to the observed phenomenon is that the quaternary ammonium cations (2Me-2HT-N^+) remained on the platelets after exfoliation of the tactoids. This would provide localized positive charges that induce their electrophoretic deposition on the negative plate.

Figure 7 provides an analysis of both types of nanoclay under comparable concentration and field strength conditions in terms of their ability to form columnar structures bridging the electrodes, i.e., the origin of the so-called "electro-viscous" effect. The microscopic images show the higher electro-responsive potential of Cloisite 15A, as previously demonstrated by viscous flow tests in Fig. 3. These results support and confirm the film forming ability of Cloisite 15A as described above.

Table 3 Minimum film thicknesses calculated according to Hamrock–Dowson (Eq. (1)), and breakdown voltages colormap (red < 5 V; orange: 5–10 V; yellow: 10–20 V; green > 20 V) for Cloisite 15A in castor oil at different concentrations

Entrainment speed (m/s)	H_m (nm)			
	Neat oil	0.5 wt%	2 wt%	4 wt%
0.50	316	360	395	423
0.75	417	474	521	557
1.00	507	577	633	678
1.25	590	671	737	789
1.50	667	760	835	893
1.75	741	844	927	991
2.00	812	924	1,015	1,086
2.25	879	1,001	1,100	1,176
2.50	945	1,075	1,181	1,264
2.75	1,008	1,147	1,260	1,348

3.3 Load-carrying capacity of the lubricant film under external electric field

Load-carrying capacity of both Cloisite 15A and Pangel B20 in castor oil was tested by a compression test in the ball-plate configuration shown in Fig. 2(b). The lubricating film was compressed while an upper ball (held at the bottom of a vertical shaft) approached a lower plate at a speed of 0.5 μm/s, from an initial height of 300 μm to the minimum achievable distance. Figure 8 shows the evolution of the axial force monitored by the rheometer transducer when the lubricant film between ball and plate was submitted to compression in an electrified tribosystem.

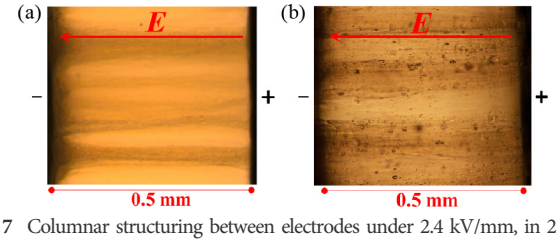

Fig. 7 Columnar structuring between electrodes under 2.4 kV/mm, in 2 wt% nanoclay in castor oil: (a) Cloisite 15A and (b) Pangel B20.

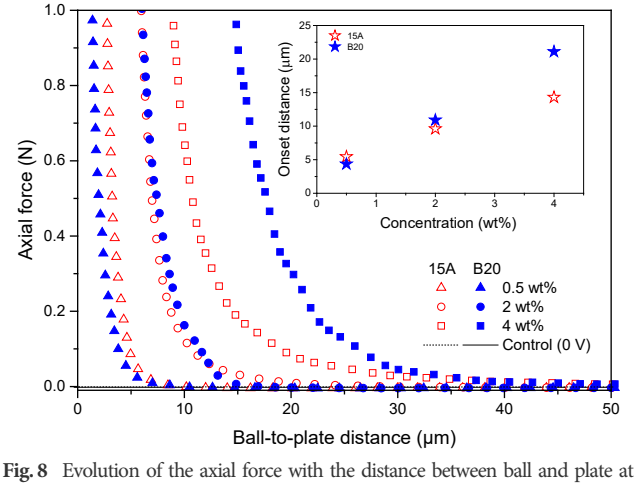

Fig. 8 Evolution of the axial force with the distance between ball and plate at 300 V for Cloisite 15A (empty symbols) and Pangel B20 (filled symbols) in castor oil. Control tests at 0 V, for reference (square symbols) (inset: onset distance vs. nanoclay concentration).

Both Cloisite 15A and Pangel B20 dispersions were evaluated at the three concentrations studied, 0.5, 2, and 4 wt%, and under an external electric voltage of 300 V. For comparison, the same tests were performed at 0 V. As can be appreciated in Fig. 8, regardless of concentration, no counterforce was detected as the ball approached the plate when no voltage was set. On the contrary, when the voltage was set to 300 V, an increasing normal force started to act on the lowering ball as the lubricant film was compressed.

This result demonstrates that the structuring of the internal morphology of the lubricant film, which consists in interfacial polarization of nanoclay particles [25], the accumulation at the contact point (Fig. 9) and subsequent arrangement into columnar structures (Fig. 7), is triggered by an external electrical stimulus. This is consistent with the fact that the electric field strength increases as the distance between electrodes (ball and plate) decreases, enhancing the electrically active structural network in the liquid. As in the ESM, a video is provided (available from https://video.uhu.es/media/Squeezing%20test/1_zj5bzu6b) showing the film behavior of the Cloisite 15A-based lubricant in an electrified tribological contact during a squeezing test at 1,000 V. The enhanced load-carrying capacity of the lubricant film (string-like structures) upon being triggered by an electrical potential is notorious (please, note how the clay mineral nanoparticles are retained by the electric field, in contrast to the nanoparticles being dragged by the oil as it flows out of the gap, in the absence of electric field). A similar conclusion was drawn by Gracia-Fernández et al. [44], using a fluid consisting of 10 wt% corn starch in silicone oil. In addition, onset distances were determined as the ball-to-plate distance at a certain value of load-change rate (first derivative of curves in Fig. 8). Such a rate was arbitrarily chosen to be 0.05 N/m. Calculated values were plotted against nanoclay concentration (inset in Fig. 8). Those values directly depend on nanoclay concentration. This result is indicative of how the load carrying capacity of the lubricant improves with increasing concentration in the presence of an electric field. B20 showed stronger dependency. In both cases, Cloisite 15A and Pangel B20, linear relationships were found within the concentration interval studied, i.e., from 0.5 to 4 wt%.

4 Conclusions

The electro-active control of friction in an electrified ball bearing prototype through fully sustainable ER lubricating fluids was analyzed. By applying an electrical voltage, the coefficient of friction could be actively adjusted as needed. Although Cloisite 15A and Pangel B20 in castor oil exhibited very different ER behavior, their ability to change the coefficient of friction was similar. In addition, it was found that the ejection of 4 wt% Pangel B20 in castor oil from the contact zone at 500 r/min was prevented when a potential difference of 1,000 V was applied. Polarized nanoparticles affected by the electric field are forced to concentrate at and around the contact point of the ball ring, preventing the oil from leaking and improving lubrication. The electric field prevented deficient lubrication and noise generation. In addition, a more stable development of the coefficient of friction over time was achieved. Cloisite 15A showed better ability than Pangel B20 to retard dielectric breakdown in castor oil. This capability is related to the electro-responsive potential, which improves film formation even at high rotation speeds. It was additionally found that the electrical potential led to structuring of the nanoclay in the lubricant so that when it was trapped between the electrified plate and the ball, it could counteract the pressure resistance. This result may have important implications for the development of fully sustainable lubricating fluids whose load-carrying capacity can be increased, if necessary, by applying an electrical voltage. Such a load-carrying capacity would allow the lubricant to operate efficiently under increasing loads without the risk of wear damage. It is not yet clear why Pangel B20 shows higher counterforce in compression test than Cloisite 15A, despite smaller viscosity change in the E-field. It was seen that the friction coefficient change is not only due to the electro-viscous effect. These promising results open up the realization of a new lubrication concept for technical applications.

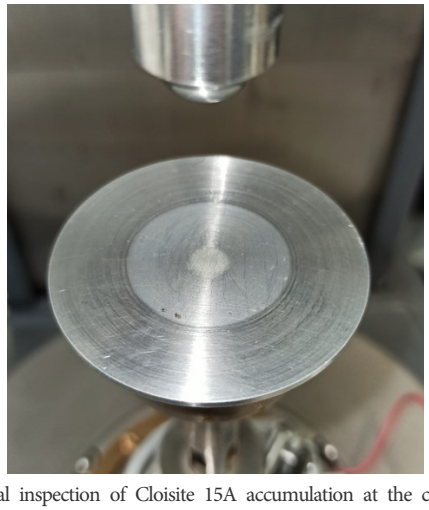

Fig. 9 Visual inspection of Cloisite 15A accumulation at the contact point between ball and plate, the point of greatest electric field strength, during compression testing.

Author contributions

Moisés García-Morales: conceptualization, methodology, writing—review & editing, supervision, project administration, and funding acquisition; Miguel Ángel Delgado: conceptualization, methodology, resources, writing—review & editing, project administration, and funding acquisition; Samuel David Fernández-Silva: methodology, validation, investigation, writing—original draft, and visualization; Claudia Roman: validation, investigation; Felix Gatti: methodology, validation, and investigation; Tobias Amann: writing—review & editing, project administration, and funding acquisition; Andreas Kailer: writing—review & editing, project administration, funding acquisition. All authors read and approved the final manuscript.

Acknowledgements

This work is part of two research projects sponsored by "Programa Operativo FEDER-Andalucía 2014-2020" (UHU-1255843 and UHU-202008), and a "Generación de Conocimiento 2023" project (PID2023-151761NB-100) funded by MICIU/AEI /10.13039/501100011033 and by FEDER, UE. The authors gratefully acknowledge their financial support. Samuel David Fernández-Silva acknowledges "Ayudas para la Contratación Predoctoral de Personal Investigador en Formación 2021, Junta de Andalucía" (PREDOC_01696), for funding his Ph.D. Thesis. In addition, it was in part also supported by Fraunhofer Cluster of Excellence Programmable Materials.

Declaration of competing interest

The authors have no competing interests to declare that are relevant to the content of this article.

Electronic Supplementary Material

Supplementary material is available in the online version of this article at https://doi.org/10.26599/FRICT.2025.9441023.

References

[1] Holmberg K, Erdemir A. Influence of tribology on global energy consumption, costs and emissions. *Friction* **5**(3): 263–284 (2017)

[2] Prashad H. Diagnosis of rolling-element bearings failure by localized electrical current between track surfaces of races and rolling-elements. *J Tribol* **124**(3): 468–473 (2002)

[3] Shah R, Chen R, Woydt M. The effects of energy efficiency and resource consumption on environmental sustainability. *Lubricants* **9** (12): 117 (2021)

[4] Asadauskas S, Perez JM, Duda JL. Lubrication properties of castor oil—Potential basestock for biodegradable lubricants. *Lubr Eng* **53**: 35–40 (1997)

[5] Ogunniyi D S. Castor oil: A vital industrial raw material. *Bioresource Technol* **97**(9): 1086–1091 (2006)

[6] Beroual A, Khaled U, Mbolo Noah P S, Sitorus H. Comparative study of breakdown voltage of mineral, synthetic and natural oils and based mineral oil mixtures under AC and DC voltages. *Energies* **10**(4): 511 (2017)

[7] Erhan S Z, Asadauskas S. Lubricant basestocks from vegetable oils. *Ind Crop Prod* **11**(2–3): 277–282 (2000)

[8] Panchal T M, Patel A, Chauhan D D, Thomas M, Patel J V. A methodological review on bio-lubricants from vegetable oil based resources. *Renew Sustain Energy Rev* **70**: 65–70 (2017)

[9] Tysoe W, Spencer ND. Rapid testing of tribotronic materials. *Tribol Lubr Technol* **77**: 76–77 (2021)

[10] Takata M, Yamaguchi T, Doi M. Friction control of a gel by electric field in ionic surfactant solution. *J Phys Soc Jpn* **79**(6): 063602 (2010)

[11] Gatti F, Amann T, Kailer A, Baltes N, Rühe J, Gumbsch P. Towards programmable friction: Control of lubrication with ionic liquid mixtures by automated electrical regulation. *Sci Rep* **10**(1): 17634 (2020)

[12] Kimura Y, Nakano K, Kato T, Morishita S. Control of friction coefficient by applying electric fields across liquid crystal boundary films. *Wear* **175**(1–2): 143–149 (1994)

[13] He Y Q, Li H, Qu C Y, Cao W, Ma M. Recent understanding of solid-liquid friction in ionic liquids. *Green Chem Eng* **2**(2): 145–157 (2021)

[14] Karuppiah KS, Zhou Y, Woo LK, Sundararajan S. Nanoscale friction switches: Friction modulation of monomolecular assemblies using external electric fields. *Langmuir* **25**(20): 12114–12119 (2009)

[15] Drummond C. Electric-field-induced friction reduction and control. *Phys Rev Lett* **109**(15): 154302 (2012)

[16] Spikes H A. Triboelectrochemistry: Influence of applied electrical potentials on friction and wear of lubricated contacts. *Tribol Lett* **68** (3): 90 (2020)

[17] He S Q, Meng Y G, Tian Y, Zuo Y H. Response characteristics of the potential-controlled friction of ZrO_2/stainless steel tribopairs in sodium dodecyl sulfate aqueous solutions. *Tribol Lett* **38**(2): 169–178 (2010)

[18] Glavatskih S, Höglund E. Tribotronics: Towards active tribology. *Tribol Int* **41**(9-10): 934–939 (2008)

[19] Krim J. Controlling friction with external electric or magnetic fields: 25 examples. *Front Mech Eng* **5**: 22 (2019)

[20] Gao Y, Xue B C, Ma L R, Luo J B. Effect of liquid crystal molecular orientation controlled by an electric field on friction. *Tribol Int* **115**: 477–482 (2017)

[21] Zhang Z, Zhu K Q. Characteristics of electrorheological fluid flow in journal bearings. *Chinese Phys Lett* **19**(2): 273–275 (2002)

[22] Nikolakopoulos P G, Papadopoulos C A. Controllable high speed journal bearings, lubricated with electro-rheological fluids. An analytical and experimental approach. *Tribol Int* **31**(5): 225–234 (1998)

[23] Gonda A, Capan R, Bechev D, Sauer B. The influence of lubricant conductivity on bearing currents in the case of rolling bearing greases. *Lubricants* **7**(12): 108 (2019)

[24] Sunahara K, Ishida Y, Yamashita S, Yamamoto M, Nishikawa H, Matsuda K, Kaneta M. Preliminary measurements of electrical micropitting in grease-lubricated point contacts. *Tribol T* **54**(5): 730–735 (2011)

[25] García-Morales M, Fernández-Silva S D, Roman C, Delgado M A. Electro-active control of the viscous flow and tribological performance of ecolubricants based on phyllosilicate clay minerals and castor oil. *Appl Clay Sci* **198**: 105830 (2020)

[26] Xie G X, Guo D, Luo J B. Lubrication under charged conditions. *Tribol Int* **84**: 22–35 (2015)

[27] Cao Z F, Xia Y Q, Xi X. Nano-montmorillonite-doped lubricating grease exhibiting excellent insulating and tribological properties. *Friction* **5**(2): 219–230 (2017)

[28] García-López D, Fernández J F, Merino J C, Santarén J, Pastor J M. Effect of organic modification of sepiolite for PA6 polymer/organoclay nanocomposites. *Compos Sci Technol* **70**(10): 1429–1436 (2010)

[29] Zhuang G Z, Zhang Z P, Yang H, Tan J J. Structures and rheological properties of organo-sepiolite in oil-based drilling fluids. *Appl Clay Sci* **154**: 43–51 (2018)

[30] Liu P F, Du M Y, Clode P, Li H L, Liu J S, Leong Y K. Surface chemisty, microstructure, and rheology of thixotropic 1-D sepiolite gels. *Clay Clay Miner* **68**(1): 9–22 (2020)

[31] Reitz R P, Plangetis G F. Bearing apparatus featuring electrorheological fluid lubrication. U.S. Patent 20 100 247 012 A1, 2010.

[32] Fernández-Silva S D, García-Morales M, Ruffel C, Delgado M A. Influence of the nanoclay concentration and oil viscosity on the rheological and tribological properties of nanoclay-based ecolubricants. *Lubricants* **9**(1): 8 (2021)

[33] Barber G C, Jiang Q Y, Zou Q, Carlson W. Development of a laboratory test device for electrorheological fluids in hydrostatic lubrication. *Tribotest* **11**(3): 185–191 (2005)

[34] Xie G, Cui Z Y, Si L N, Guo D. Destabilization of lubrication oil micropool under charged conditions. *Ind Lubr Tribol* **69**: 59–64 (2010)

[35] Roman C, García-Morales M, Goswami S, Marques A C, Cidade M T. The electrorheological performance of polyaniline-based hybrid particles suspensions in silicone oil: Influence of the dispersing medium viscosity. *Smart Mater Struct* **27**(7): 075001 (2018)

[36] Jablonka K, Glovnea R, Bongaerts J. Quantitative measurements of film thickness in a radially loaded deep-groove ball bearing. *Tribol Int* **119**: 239–249 (2018)

[37] Shetty P, Meijer R J, Osara J A, Lugt P M. Measuring film thickness in starved grease-lubricated ball bearings: An improved electrical capacitance method. *Tribol T* **65**(5): 869–879 (2022)

[38] Hamrock B J, Dowson D. Isothermal elastohydrodynamic lubrication of point contacts: Part 1—Theoretical formulation. *J Lubr Technol* **98**(2): 223–228 (1976)

[39] Hamrock B J, Dowson D. Isothermal elastohydrodynamic lubrication of point contacts: Part III: Fully flooded results. *J Lubr Technol* **99**: 264–275 (1977)

[40] Hamrock B J, Dowson D, Tallián T E. Ball bearing lubrication: The elastohydrodynamics of elliptical contacts. *J Lubr Technol* **104**(2): 279–281 (1982)

[41] Ohno N, Mori H, Mawatari T, Zhang B, Ono B. Prediction of pressure-viscosity coefficient of environmentaly friendly vegetable oils from adiabatic bulk modulus based on sound velocity under atmospheric pressure. In: Proceedings of the ASIATRIB, Agra, India, 2014: 1–3.

[42] Biresaw G, Bantchev G B. Pressure viscosity coefficient of vegetable oils. *Tribol Lett* **49**(3): 501–512 (2013)

[43] Liang J J, Wei J C, Lee Y L, Hsu S H, Lin J J, Lin Y L. Surfactant-modified nanoclay exhibits an antiviral activity with high potency and broad spectrum. *J Virol* **88**(8): 4218–4228 (2014)

[44] Gracia-Fernández C, Gómez-Barreiro S, Álvarez-García A, López-Beceiro J, Artiaga R. Electrorheological behaviour of a starch-oil system. *Rheol Acta* **53**(8): 655–661 (2014)

Samuel David Fernández-Silva holds his B.Sci. degree in chemistry (2017) and M.Eng. degree in chemical engineering (2021), both of them awarded by the University of Huelva, Spain. He has recently finished his doctoral studies, also at the University of Huelva. His Ph.D. Thesis was devoted to explore the development of functional nanocellulose-based and nanoclay mineral-based biolubricants, with a view to the electro-active control of the friction behavior, both in simple ball-on-three plates setups and more specialized tribological contacts such as ball bearings.

Moisés García-Morales received his M.Eng. (2001) and Ph.D. (2005) degrees in chemical engineering from the University of Huelva, Spain. Currently, he is a full professor at the department of chemical engineering, at the same institution. His research interests mainly include the use of nanotechnology as a sustainable approach for assuring the environment preservation. In that sense, he is involved in several projects which deal with the active control of lubrication through electro-triggering and sustainable nanofluids, as well as the development of ecofriendly lubricating oleogels based on nanocellulose and vegetable oils.